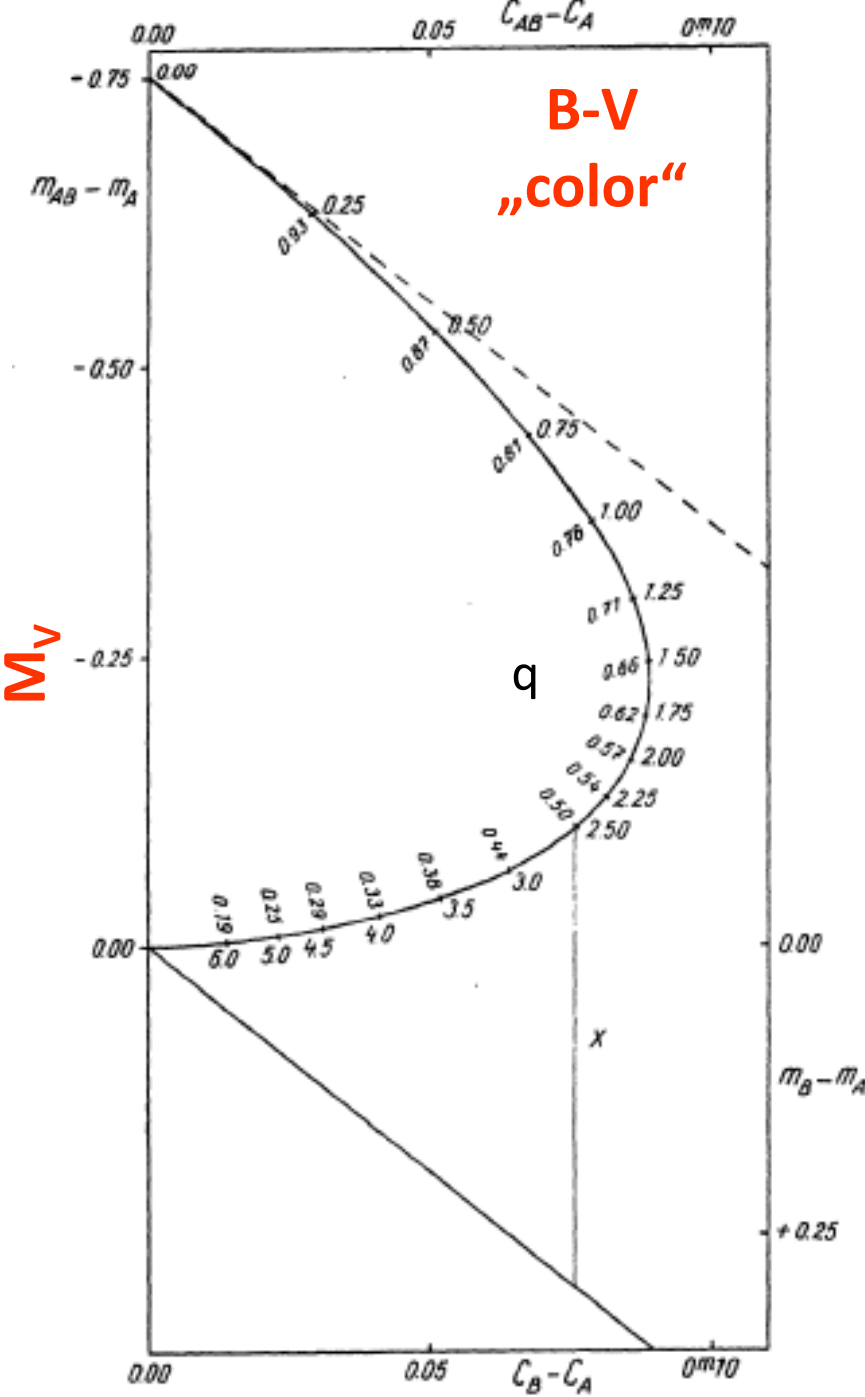Hyades

log t = 8.90
d = 45 pc
[Fe/H] = +0.17 dex

Width of Main Sequence
about 1.8 mag in M_V

NO
Observational error

What are the reasons?

B-V „color"

Vertical distance from the main sequence

$$x = a(C_{AB} - C_A) + V_A - V_{AB}$$

Absolute magnitude:

$$M_V = -2.5 \log (L_1 + L_2)$$
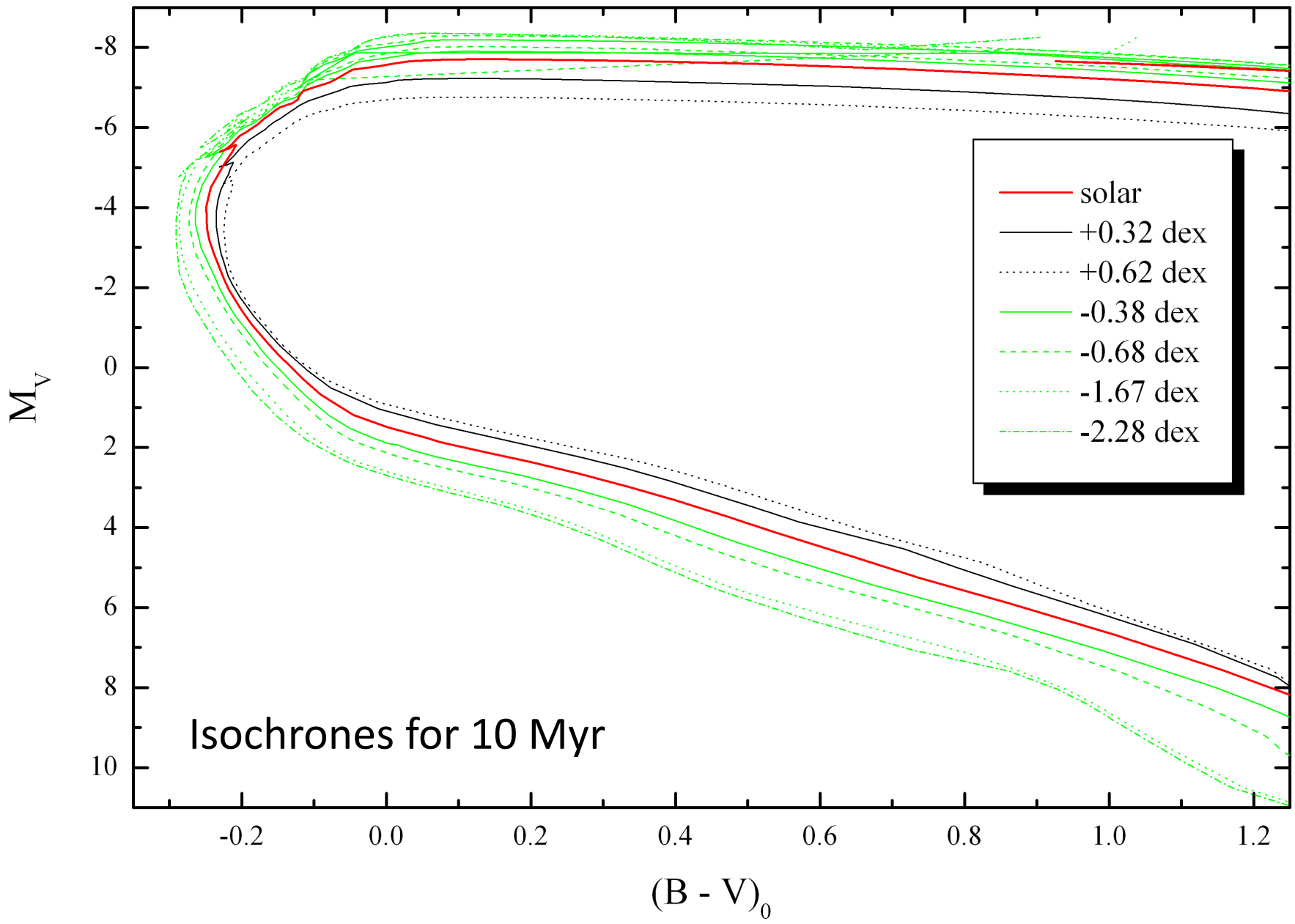
Maximum at $L_1 = L_2$ =>

$$M_V = -0.753 \text{ mag}$$

The maximal width of the main sequence due to binary systems is 0.753 mag

Haffner & Heckmann, 1937, VeGeo, 55, 77

Praesepe: Fossati et al., 2008, A&A, 483, 891

At.N.	Element	HD 72846	HD 73345	HD 73450	"Normal" A-type stars HD 73574	HD 74028	HD 74050	HD 74587	HD 74718	Solar Abundances
3	Li	< −8.08(−; 1)	< −8.33(−; 1)	< −8.70(−; 1)	< −8.38(−; 1)			< −8.41(−; 1)	< −8.26(−; 1)	−10.99
6	C	−3.58(−; 1)	−3.44(12; 3)	−3.27(−; 1)	−3.36(18; 2)	−3.39(08; 2)	−3.52(−; 1)	−3.49(01; 2)	−3.51(04; 2)	−3.65
8	O	−3.18(−; 1)	−3.22(01; 2)				−3.70(−; 1)	−3.30(−; 1)		−3.38
11	Na	−5.44(01; 2)	−5.37(01; 2)	−6.28(−; 1)	−5.57(02; 2)	−5.98(−; 1)	−5.64(13; 2)	−5.61(02; 2)	−5.70(14; 2)	−5.87
12	Mg	−4.18(08; 3)	−4.18(02; 3)	−5.02(18; 2)	−4.37(04; 3)	−4.86(08; 3)	−4.22(05; 4)	−4.56(08; 3)	−4.52(01; 2)	−4.51
14	Si	−4.62(16; 2)	−4.67(−; 1)	−4.13(−; 1)	−4.19(−; 1)	−4.17(−; 1)	−4.37(−; 1)	−4.16(−; 1)	−4.25(−; 1)	−4.53
16	S	−4.71(04; 2)	−4.44(03; 4)	−4.35(−; 1)	−4.61(02; 2)	−4.26(01; 2)		−4.50(04; 2)	−4.28(11; 2)	−4.90
20	Ca	−5.17(−; 1)	−5.39(09; 6)	−5.95(06; 4)	−5.86(16; 5)	−5.37(16; 2)	−6.13(06; 2)	−5.49(15; 6)	−5.68(02; 3)	−5.73
21	Sc	−8.88(−; 1)	−8.63(07; 3)	−8.57(14; 3)	−8.89(02; 3)	−8.35(−; 1)	−8.96(27; 3)	−8.56(−; 1)	−8.69(14; 2)	−8.99
22	Ti	−6.88(03; 5)	−6.95(06; 6)	−7.30(11; 5)	−6.98(09; 5)	−6.78(−; 1)	−7.08(15; 5)	−6.83(16; 3)	−6.93(10; 5)	−7.14
24	Cr	−6.23(06; 3)	−6.22(08; 2)	−6.56(08; 3)	−6.19(16; 3)	−6.23(12; 4)	−6.48(10; 3)	−6.05(13; 4)	−6.44(20; 5)	−6.40
25	Mn		−6.37(−; 1)	−6.88(−; 1)	−6.52(02; 2)	−6.77(−; 1)	−6.61(−; 1)	−6.62(04; 2)	−6.71(−; 1)	−6.65
26	Fe	−4.55(18; 42)	−4.33(11; 61)	−4.62(09; 15)	−4.49(10; 30)	−4.50(09; 18)	−4.44(13; 16)	−4.28(10; 33)	−4.61(11; 26)	−4.59
28	Ni	−5.70(18; 2)	−5.58(11; 4)	−5.82(16; 2)	−5.62(08; 4)	−5.93(14; 3)	−5.60(15; 3)	−5.84(−; 1)	−5.68(02; 3)	−5.81
39	Y	−9.75(−; 1)	−9.46(−; 1)	−9.83(−; 1)	−9.20(−; 1)	−9.56(−; 1)	−9.26(−; 1)	−9.13(−; 1)	−9.10(−; 1)	−9.83
56	Ba	−9.48(−; 1)	−9.30(06; 2)	−9.50(02; 2)	−8.98(04; 2)	−9.65(−; 1)	−9.52(01; 2)	−8.96(25; 2)	−9.15(−; 1)	−9.87
	T_{eff}	8045	7993	7270	7662	7750	7872	7500	7600	
	$\log g$	3.50	3.96	4.20	4.00	4.50	3.66	4.20	4.00	
	v_{mic}	2.5	2.6	2.7	2.6	2.6	2.6	2.7	2.7	
	$v \sin i$	119	85	138	102	150	188	90	155	

Fe: -4.28 to -4.62dex; 0.34 dex

Metallicity => different opacity

Isochrones for 10 Myr

Legend:
- solar
- +0.32 dex
- +0.62 dex
- -0.38 dex
- -0.68 dex
- -1.67 dex
- -2.28 dex

Axes: M_V (vertical), $(B - V)_0$ (horizontal)

Rotation

$T_e = 35,880°K$ $\log g = 4.10$
Pole
$T_e = 34,750°K$ Latitude 60° $\log g = 4.04$
$T_e = 33,340°K$ Latitude 45° $\log g = 3.97$
$T_e = 31,410°K$ Latitude 30° $\log g = 3.87$

$T_e = 28,110°K$ $\log g = 3.67$ V (equatorial) = 417 km/sec
Equator

BO Model
w = 0.9
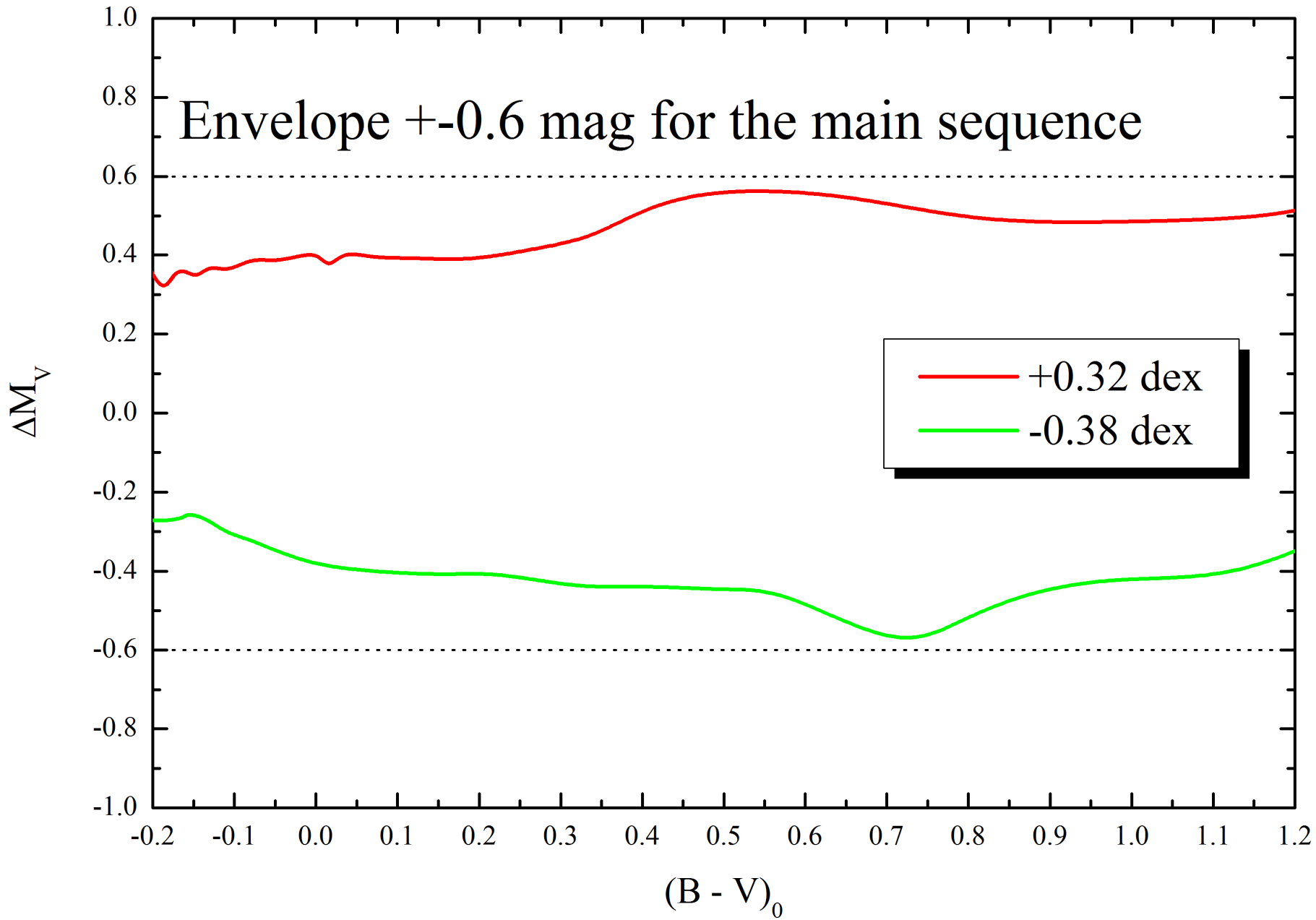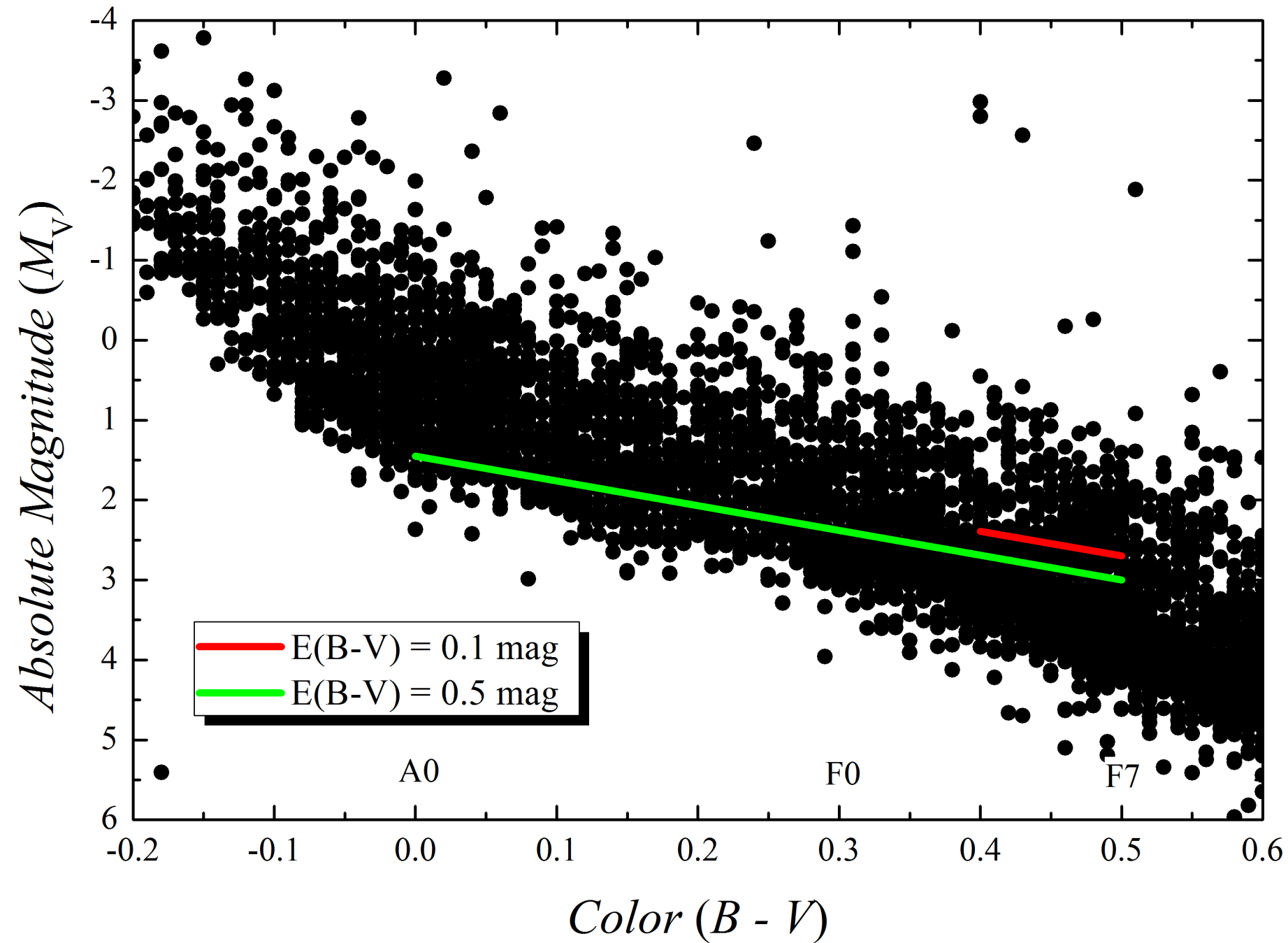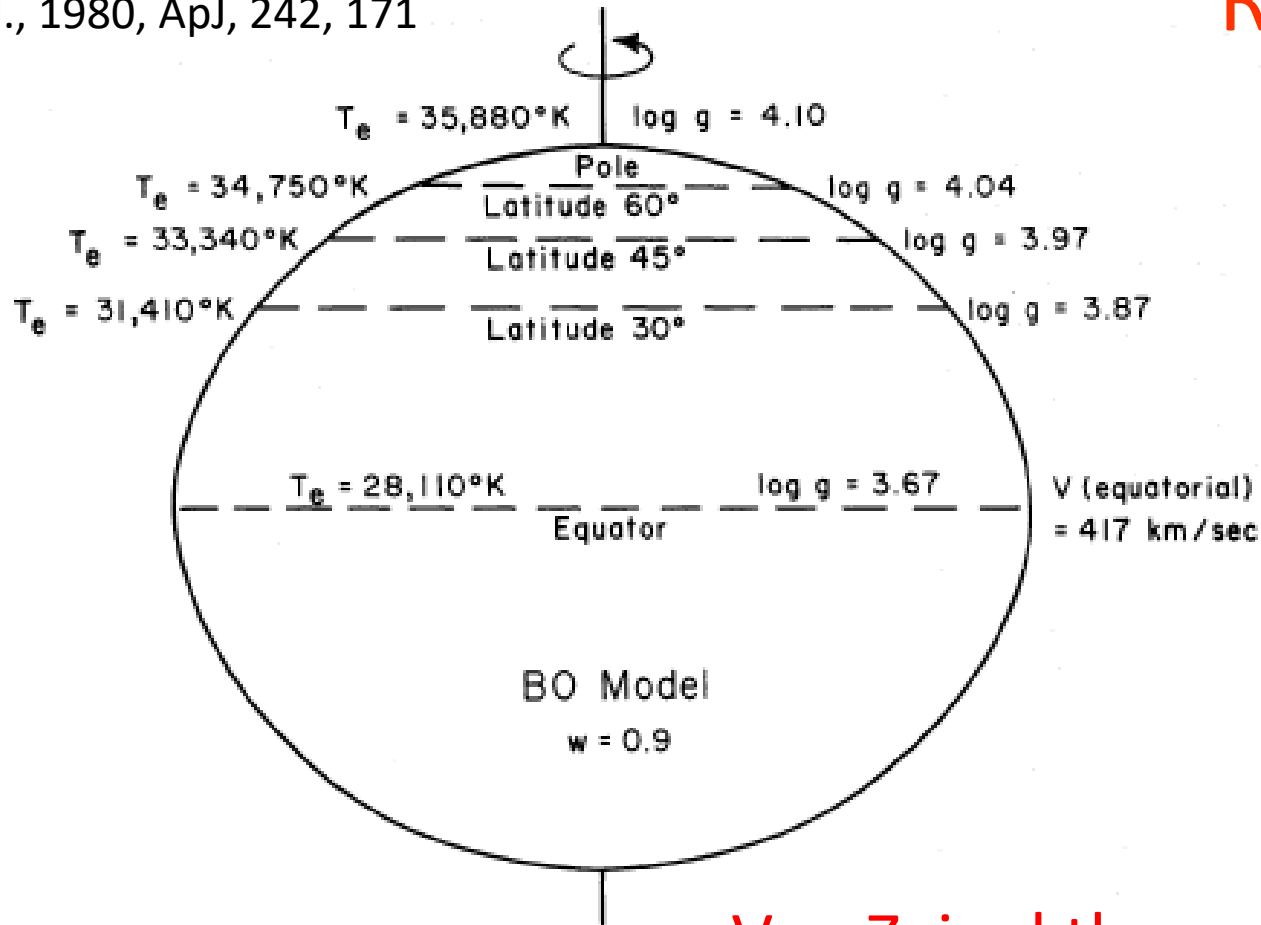
Von Zeipel theorem (1924, MNRAS, 84, 665)

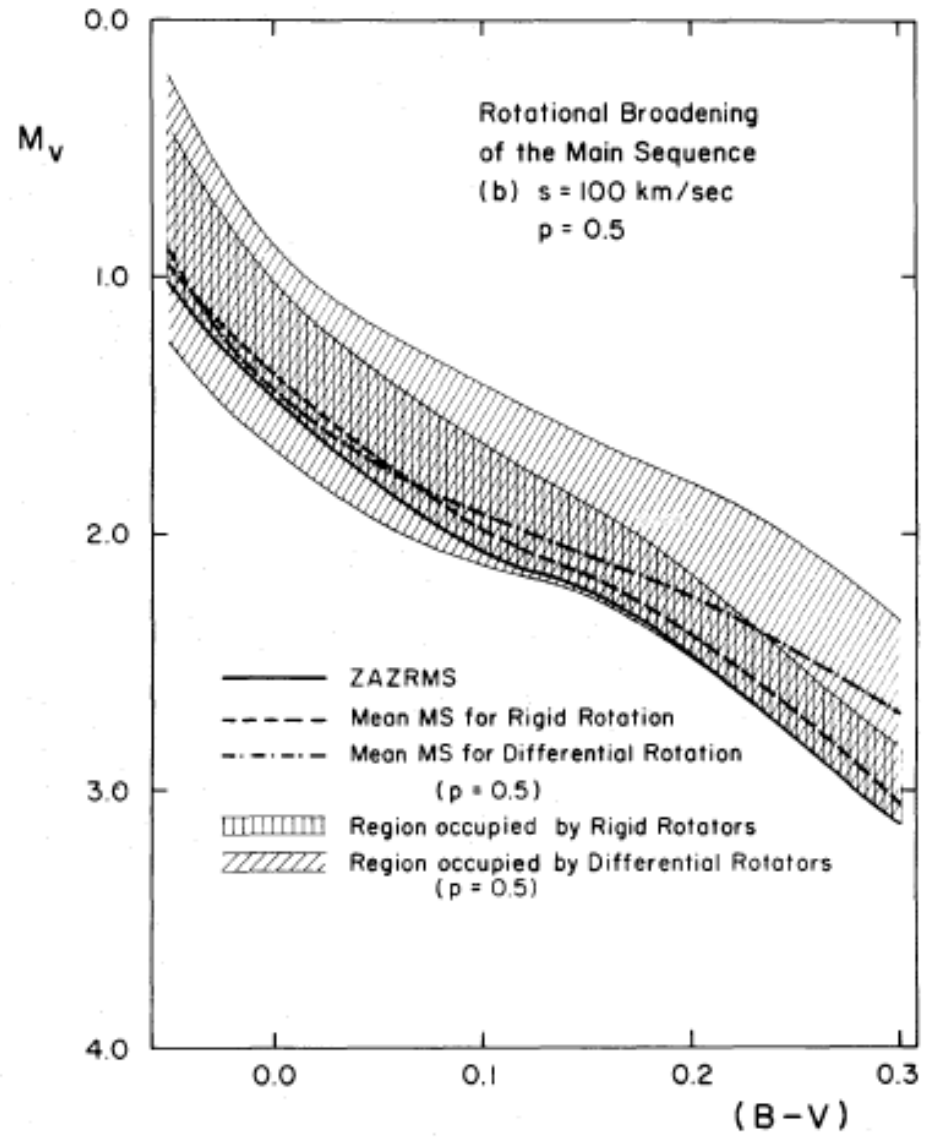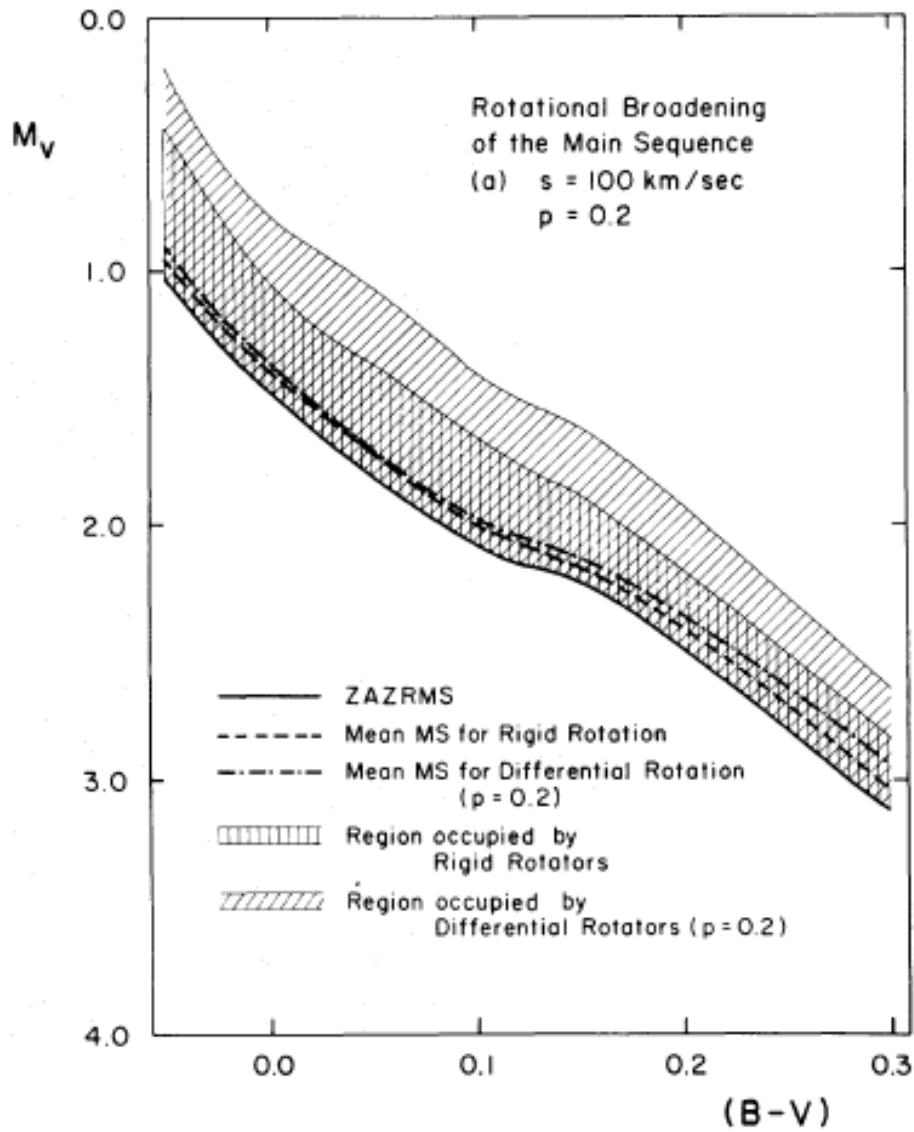Energy generation rate $\epsilon = (\text{const})\left(1 - \dfrac{\omega^2}{2\pi G\rho}\right)$

From the rotational velocity => ε => T_{eff} and L (log g)

Vega

Table 7

A Summary of Physical Parameters for the Pole-on Model

Parameter	Value
Equatorial radius ($R_\odot$)	2.75 ± 0.01
Polar radius ($R_\odot$)	2.40 ± 0.02
Polar effective temperature (K)	10000 ± 30
Pole-to-equator $T_{\rm eff}$ difference (K)	1410
Mean effective temperature (K)	9560 ± 30
Luminosity ($L_\odot$)	44 ± 2
Mass ($M_\odot$)	2.4 ± 0.1
Polar surface gravity (cgs, dex)	4.04 ± 0.01
Pole-to-equator $\log g$ difference (cgs, dex)	0.26
Mean surface gravity (cgs, dex)	3.95 ± 0.01
Projected rotational velocity (km s^{-1})	20.8 ± 0.2
Inclination of rotation axis (degrees)	5.7 ± 0.1
Equatorial rotational velocity (km s^{-1})	211 ± 4
Fraction of breakup velocity (km s^{-1})	$0.81 \pm .02$

Hill et al., 2010, ApJ, 712, 250

Collins & Smith, 1985, MNRAS, 213, 519

p … Degree of differential rotation

Figure (a): Johnson Colours, Rotational Broadening of the Main Sequence. (a) s = 100 km/sec, p = 0.2. ZAZRMS; Mean MS for Rigid Rotators; Mean MS for Differential Rotators (p = 0.2); Region occupied by Rigid Rotators; Region occupied by Differential Rotators (p = 0.2).

Figure (b): Johnson Colours, Rotational Broadening of the Main Sequence. (b) s = 100 km/sec, p = 0.5. ZAZRMS; Mean MS for Rigid Rotators; Mean MS for Differential Rotators (p = 0.5); Region occupied by Rigid Rotators; Region occupied by Differential Rotators (p = 0.5).

Conclusions – Width of the Main Sequence

- Differential reddening: $k \cdot \Delta E(B\text{-}V)$

- Spectroscopic Binaries: 0.753 mag

- Metallicity: up to 1.2 mag for M_V, but only 0.2 mag for $(U - B)$ versus $(B - V)$

- Rotation: 1 mag for M_V, 0.2 (?) mag for $(U - B)$ versus $(B - V)$

Binary fraction

- Important for the formation and evolution of star clusters

- Critical parameter for the IMF

- Needed for N-body numerical simulations

- Observations are biased in many respects

- Many different types of binary systems
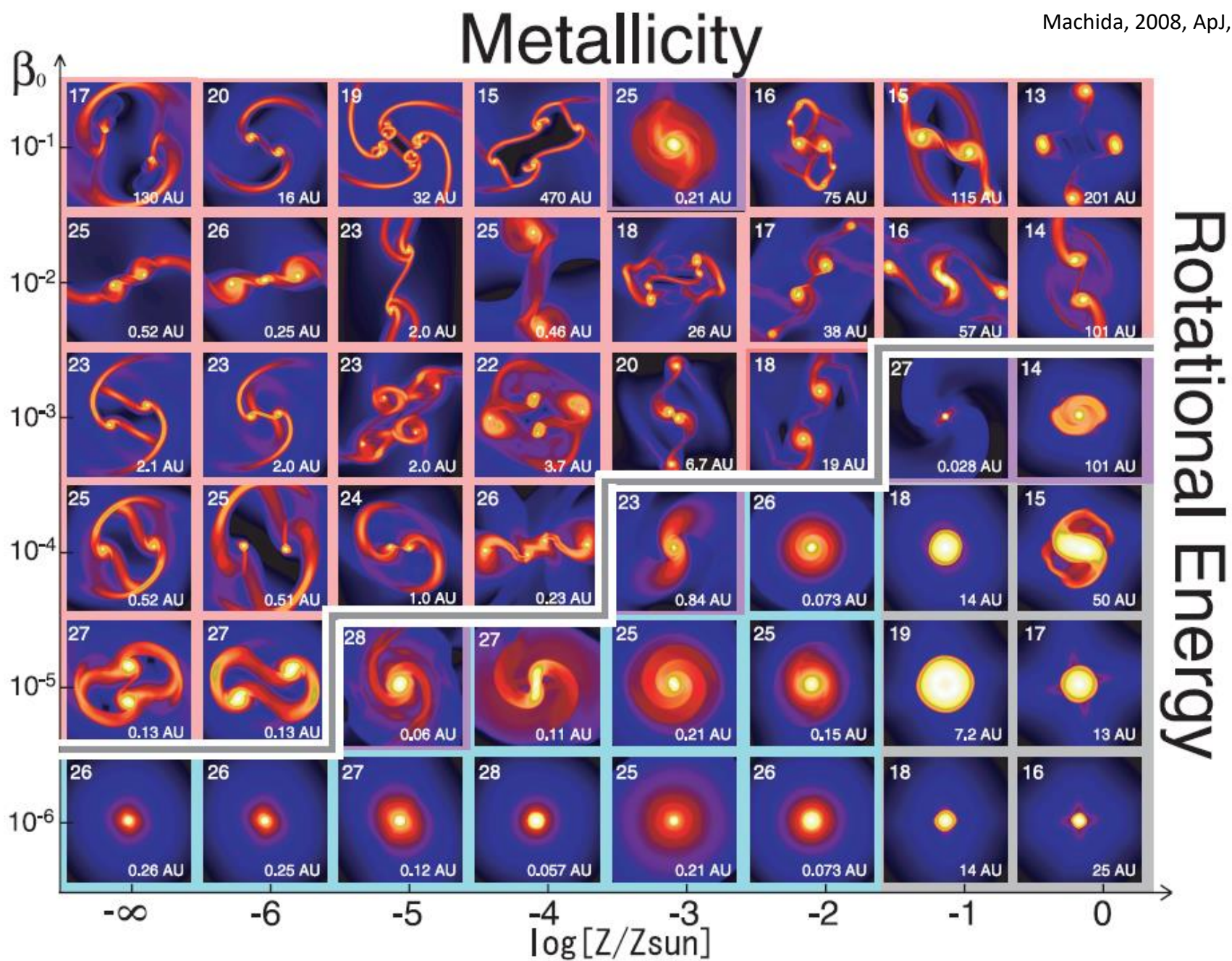
Lower metallicities seem to favour binary formation

How to observe the binary fraction?

- Photometric observations of star clusters
  1. "Cluster main sequence"
  2. Eclipsing binaries
  3. Positions (astrometric binaries)
- Spectroscopic observations
  1. Radial velocity variability
  2. Direct detection in spectrum (SB2)
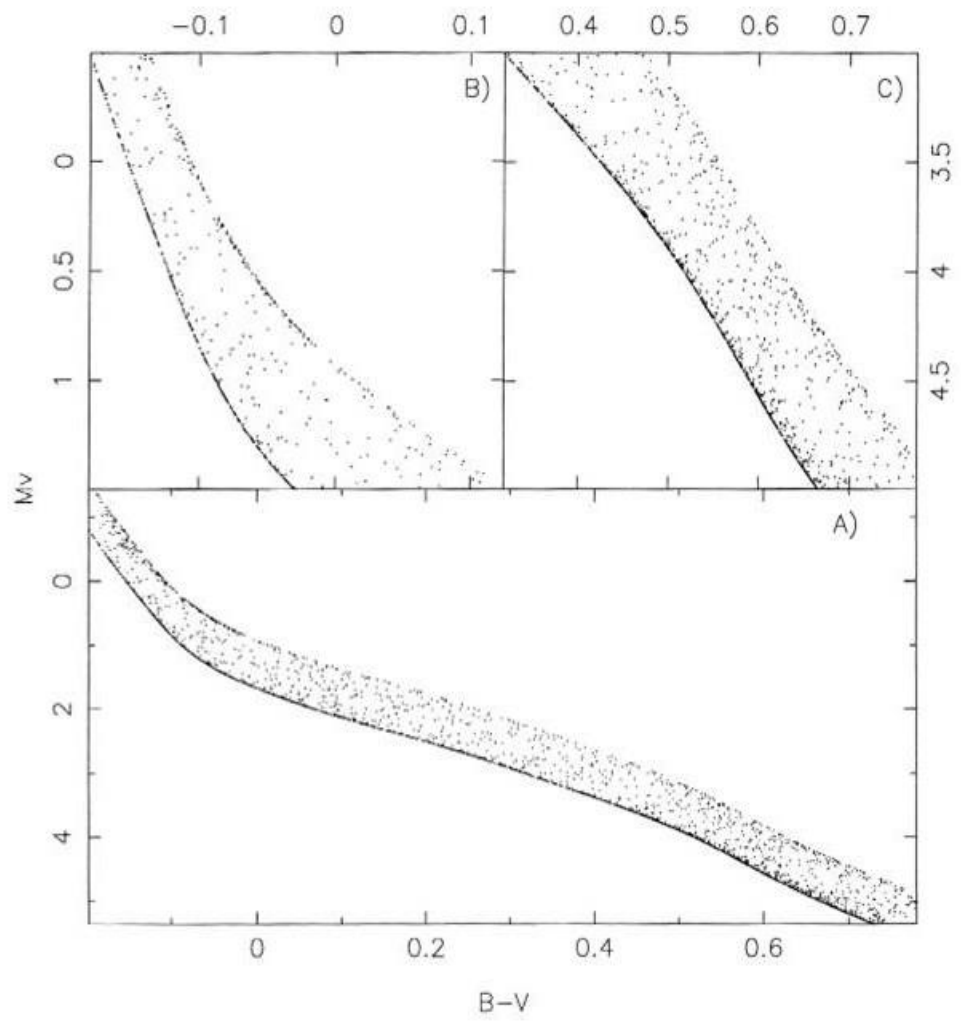
Simulation with randomly distributed mass ratios
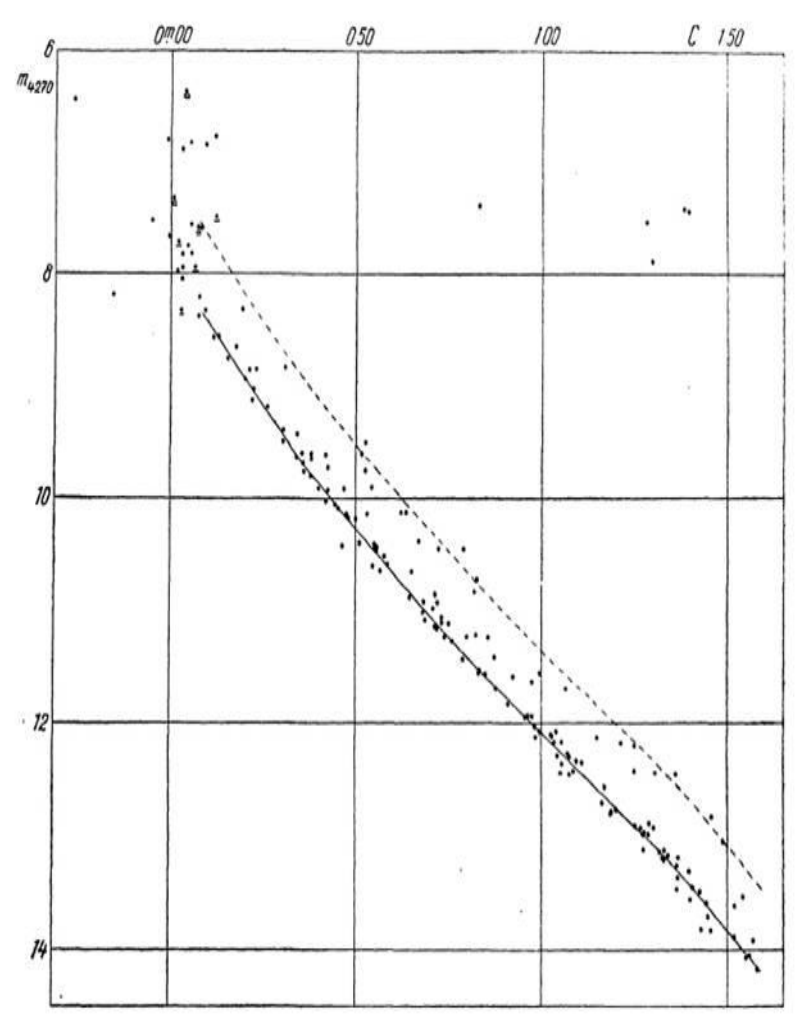
Observations of Praesepe with known binary systems

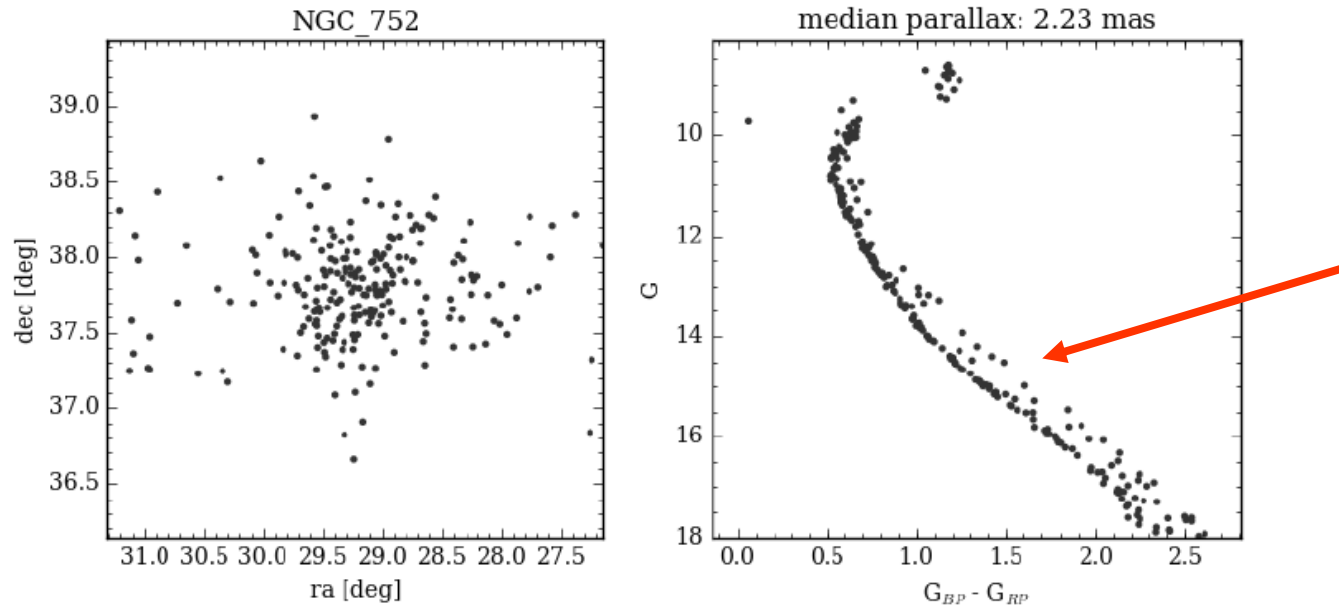# Observed binaries with the Gaia DR2

Fig. A.11. Left: distribution of the probable members of NGC 752. Right: colour-magnitude diagram of the probable members.

Cantat-Gaudin et al., 2018, A&A, 618, A93
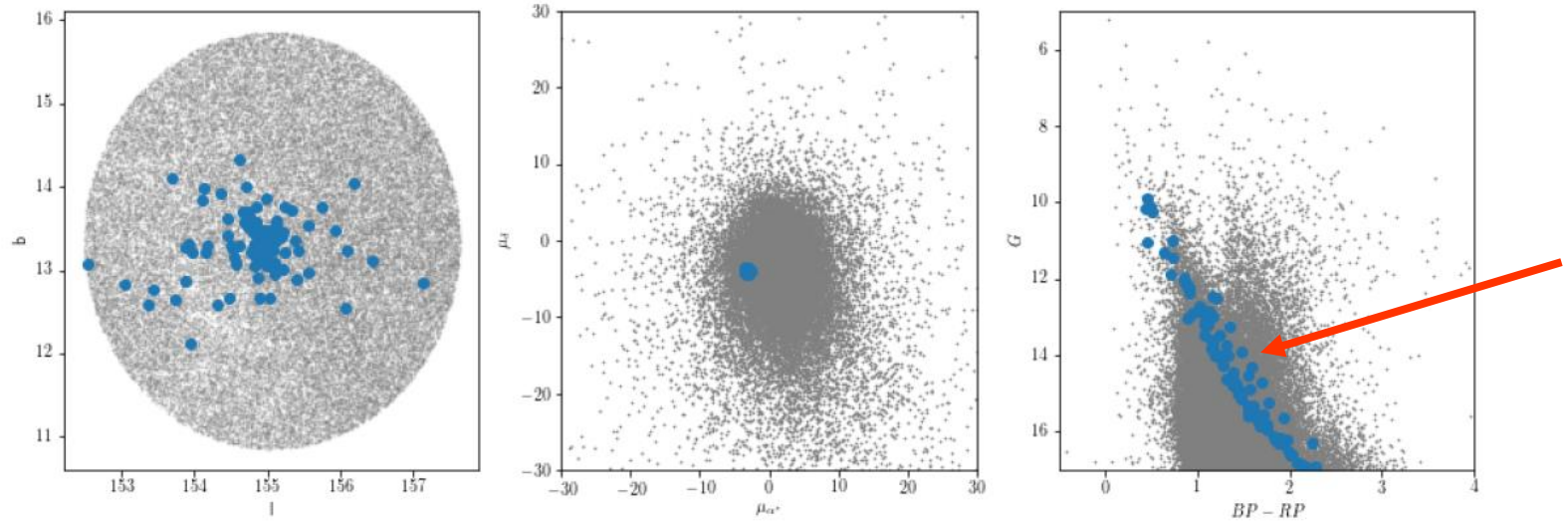
Observed binaries with the Gaia DR2

Fig. A.8: Member stars (blue) together with field stars (grey) for UBC8 in (l, b) (left) and in proper motion space (middle). The Color-Magnitude Diagram shows the sequence of the identified members (outlining an empirical isochrone) (right).
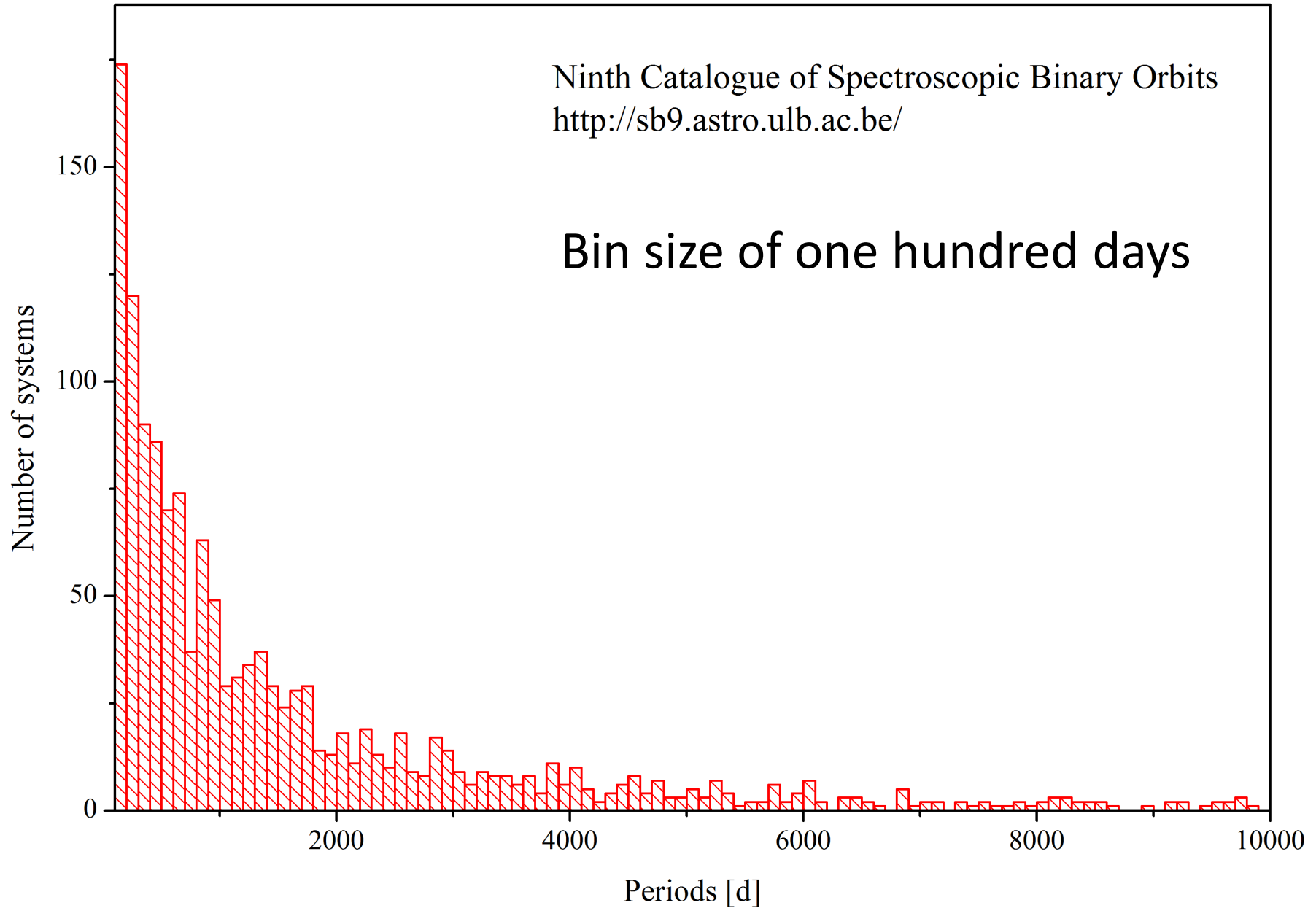
Cantat-Gaudin et al., 2018, A&A, 618, A59

Ninth Catalogue of Spectroscopic Binary Orbits
http://sb9.astro.ulb.ac.be/

Bin size of one day

Ninth Catalogue of Spectroscopic Binary Orbits
http://sb9.astro.ulb.ac.be/
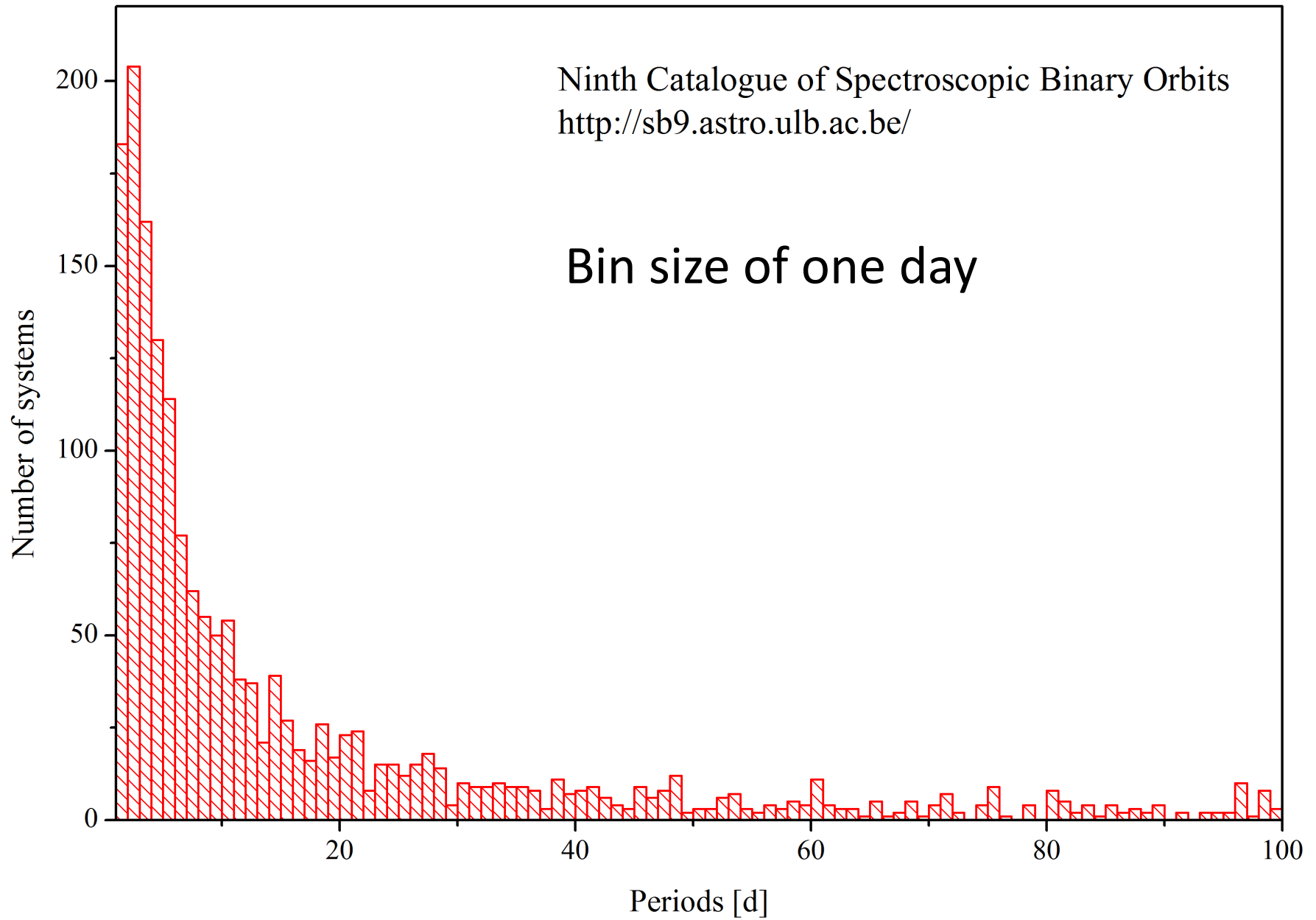
Bin size of one hundred days
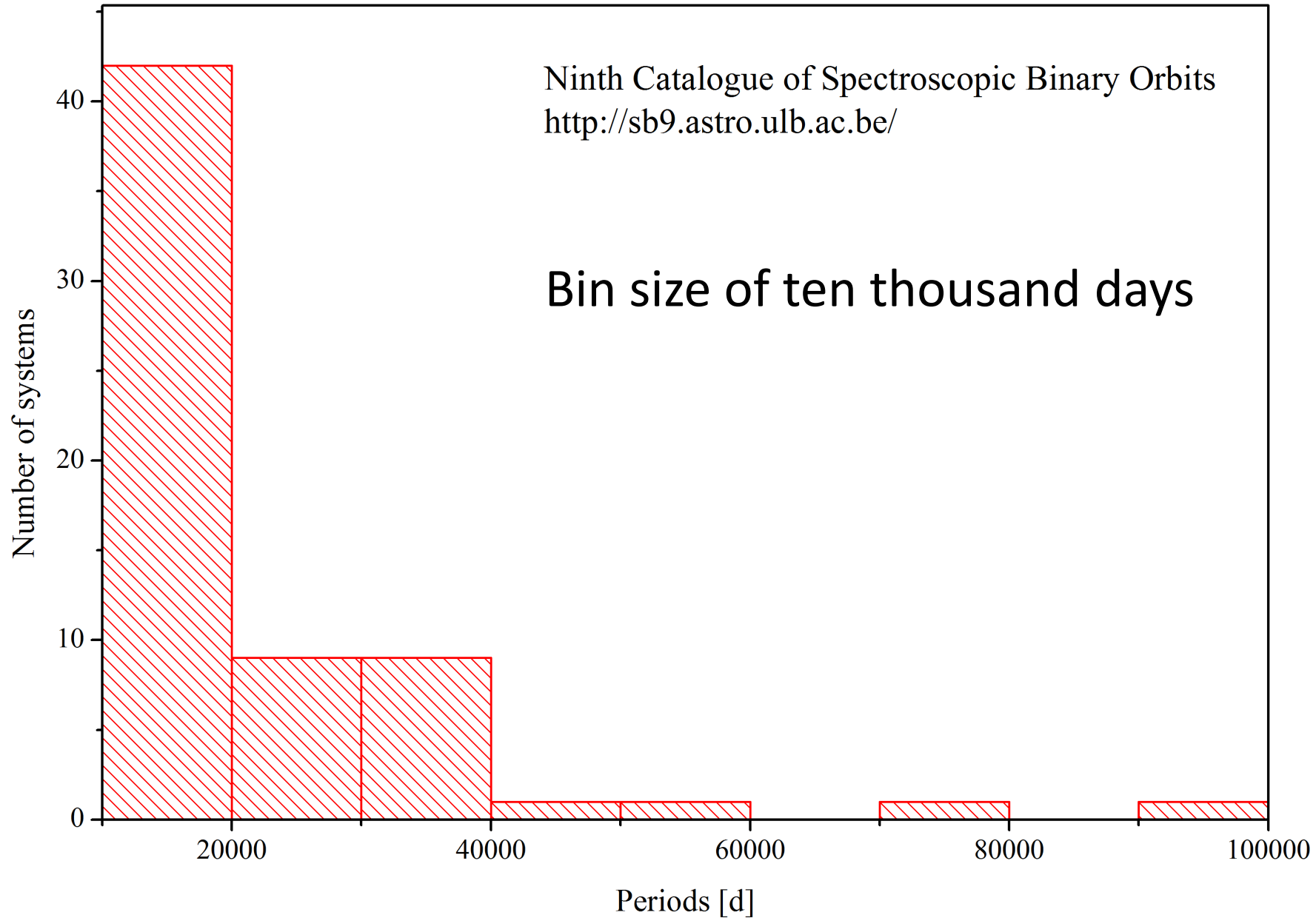
Results for open clusters

- Sollima et al., 2010, MNRAS, 401, 577
  - NGC 188 (9.63): 21 – 58%
  - NGC 2204 (9.20): 12 – 36%
  - NGC 2243 (9.58): 34 – 70%
  - NGC 2420 (9.08): 17 – 51%
  - NGC 2516 (8.52): 25 – 66%
- Sana et al., 2009, MNRAS, 400, 1479
  - NGC 6611 (6.50): 44 – 67%
- Sana et al., 2008, MNRAS, 386, 447
  - NGC 6231 (6.50): 63% - ?

- Bica & Bonatto, 2005, A&A, 431, 943
  - IC 4651 (9.26): 50 +- 11%
  - NGC 2287 (8.20): 48 +- 45%
  - NGC 2447 (8.60): 21 +- 9%
  - NGC 2548 (8.56): 48 +- 23%
  - NGC 2682 (9.51): 39 +- 16%
  - NGC 3680 (9.20): 25 +- 5%
  - NGC 5822 (9.00): 16 +- 8%
  - NGC 6208 (9.11): 54 +- 30%
  - NGC 6694 (7.85): 18 +- 12%
- Sandhu et al., 2003, A&A, 408, 515
  - NGC 2099 (8.60): ~30%
  - King 5 (9.00): ~30%
  - King 7 (8.80): ~20%

	f		
NGC 288	0.15 ± 0.05	M3	
	>0.06		
NGC 362	0.21 ± 0.06		0.14 ± 0.08
NGC 2808		M4	$0.23^{+0.34}_{-0.23}$
NGC 3201		M15	~ 0.07
NGC 4590	>0.09	M22	
NGC 5053	>0.08	M30	
NGC 5466	>0.08	M55	>0.06
NGC 5897	>0.07	M71	$0.22^{+0.26}_{-0.12}$
NGC 6101	>0.09	M92	
NGC 6362	>0.06	Arp 2	>0.08
NGC 6397	<0.07	Terzan 7	>0.21
NGC 6723	>0.06	Palmoar 12	>0.18
NGC 6752	0.27 ± 0.12	Palmoar 13	0.30 ± 0.04
NGC 6792		47 Tucane	0.14 ± 0.04
NGC 6981	>0.10		

Davis et al., 2008, AJ, 135, 2155